European Spine Journal
https://doi.org/10.1007/s00586-026-10243-5

RESEARCH

Not just alignment: body shape influences adult spinal deformity biomechanics

Elisa R. Rosanò[1,2] · Abdul Hulleck[3] · Tao Liu[4] · Marwan El-Rich[3] · Markus Loibl[5] · Fabio Galbusera[5] · Frank Kleinstück[5] · Tamas Fekete[5] · Daniel Haschtmann[5] · Sarah Richner-Wunderlin[5] · Ferran Pellisé[6] · Ibrahim Obeid[7] · Javier Pizones[8] · Ahmet Alanay[9] · Caglar Yilgor[10] · Luigi La Barbera[1] · Stephen J. Ferguson[2] · Dominika Ignasiak[2] · ESSG European Spine Study Group

Received: 15 April 2026 / Revised: 22 June 2026 / Accepted: 28 July 2026
© The Author(s) 2026

Abstract

Purpose Adult spinal deformity (ASD) alters sagittal alignment and trunk centre of mass location, increasing spinal loading. Current clinical assessment of ASD primarily focuses on alignment parameters disregarding patient's body shape variability. This study aimed to evaluate the relative effects of spinal sagittal alignment and body mass distribution (i.e., body shape) on spinal loads and trunk centre of mass location in upright-posture and forward flexion.

Methods Sagittal alignments of 754 patients with ASD were obtained from clinical data. Trunk mass distributions were assessed in adult male volunteers (10 healthy weight, 9 obese). Using an established musculoskeletal model of the spine, inverse dynamics simulations were performed for each combination of sagittal alignment and trunk mass distribution profile. A factorial analysis using generalised linear models elucidated the relative effects of alignment vs. body shape.

Results Sagittal alignment primarily determined the antero-posterior positioning of trunk centre of mass; body shape, its cranio-caudal location. In the healthy weight cohort, the relative effect of mass distribution on compressive loads was 14–98% in the thoracic and 42–57% in the lumbar region. In the cohort with obesity, it was 24–98% and 19–27%, for thoracic and lumbar regions, respectively. Body shape effects on shear forces were greater in dynamic forward flexion than in static upright-posture.

Conclusion The considerable impact of mass distribution on spinal loads suggests that patient body shape should be considered in ASD surgical planning to avoid segmental overloading. Future research should evaluate body shapes in patients with ASD, including females and elderly subjects.

Keywords Spine biomechanics · Musculoskeletal simulation · Adult spinal deformity · Sagittal alignment · Body shape · Generalised linear models

Introduction

Adult spinal deformity (ASD) encompasses disorders characterised by abnormal spinal curvature, affecting up to 68% of individuals over 65 [1]. Age-related degeneration frequently leads to positive sagittal balance [2, 3] with a forward shift of the body's centre of mass (CoM), increasing muscular demands [4], fatigue and pain [5, 6]. Optimal spine biomechanics assumes the CoM balanced over the pelvis, slightly behind the femoral heads in front of the S2 vertebra [2, 7], as more generally in Dubousset's cone of economy [8]. This rationale drives ASD surgical correction [9] aimed at realigning sagittal curvature, restoring ergonomic posture, and relieving symptoms [7]. However, mechanical complications (e.g., proximal/distal junctional and implant-related) occur in 28–61% of cases [10], with 12–35% requiring revision surgery [10]. Higher body mass index (BMI) [11], particularly obesity (BMI $\geq$ 30 kg/m^2 [12]), increases both complications [13] and revision risk [14]. Since current sagittal alignment targets may not guarantee optimal spinal balance and biomechanics, improved preoperative planning of ASD surgery is strongly needed.

Extended author information available on the last page of the article

Published online: 01 August 2026

What is disregarded in ASD clinical assessment is the inter-individual variability in body shape.

Body shape, characterised by anthropometric dimensions and body proportions, varies between individuals even with similar BMI. Empirical classifications [15] and analytical methods [16–18] highlight profound population-level body shape differences. Broad ranges of hip, waist, and chest dimensions [19], as well as hip-to-waist ratio [20, 21], reflect trunk shape diversity from hourglass or pear-shaped to apple-shaped. Body shape taxonomies have been distinguished [15, 22], describing weight accumulation patterns (e.g., rounded, rectangle, triangle, inverted triangle) and distance-based proportions (e.g., trunk vs. leg length, shoulder vs. hip width [15]). While relevant in the apparel industry [22], ergonomics [23, 24], and for health status [25], body shape's biomechanical consequences for spine surgery remain unexplored.

Musculoskeletal (MSK) modelling studies investigating ASD biomechanics reported that spinal loads depend on spinal alignment and corrective surgery [26–28], and approximately linearly on body mass (BM) [29, 30]. However, across various studies, body mass distribution along the spinal column is typically scaled uniformly [31–33]. This assumption neglects interpersonal variability in body shape parameters (BSPs), i.e., positions of CoMs and masses associated with spinal levels, as well as inertia moments. Variations in BSPs might affect overall body CoM and were shown to impact MSK model spinal loads predictions [34]. This implies that identical sagittal alignment and BMI may represent different biomechanics depending on BSPs [34]. While personalized spine MSK models have emerged to investigate patient-specific sagittal alignment and BSPs [35, 36], their relative impact on spinal loads, relevant in ASD, remains unknown.

The aim of this study is to investigate the relative effects of spinal sagittal alignment and body shape (trunk mass distribution) on model-predicted spinal segmental loads and trunk CoM location in patients with ASD, during static upright-posture and dynamic forward flexion. The second objective is to evaluate errors in spinal loads prediction from ignoring body morphology. We hypothesised that mass distribution substantially affects spinal loads and that body morphology influences spinal balance, defined by the antero-posterior (A-P) location of trunk CoM. To test these hypotheses, an established MSK model of the spine [28] was used to generate synthetic cohorts, calculate CoM, and simulate spinal loads, while generalised linear models (GLMs) enabled factorial analysis.

Methods

Patient dataset

A retrospective dataset comprising 754 patients diagnosed with ASD was utilised for this study. Data were gathered as part of the multi-centre prospective study conducted by the European Spine Study Group (ESSG), a collaboration of 6 clinical sites across Europe (Barcelona, Bordeaux, Istanbul, Madrid, Strasbourg, Zurich). The following criteria were employed for patient enrolment in the database: age of $\geq$18 years and at least 1 of the following: coronal Cobb angle$\geq$20°, sagittal vertical axis (SVA) of $\geq$5 cm, pelvic tilt (PT) of $\geq$25°, or thoracic kyphosis (TK) of $\geq$60°. For the present study, only patients without prior spinal surgery were selected. Additional exclusion criteria addressed study's simulation requirements: cases with missing data essential for patient alignment reconstruction (incomplete alignment data, no available calibration ruler, incomplete annotation), simulation errors (failed kinematics, incomplete dynamic simulations), and non-physiological muscle activation (peak muscular activity$>$90%), reflecting inability of the model to simulate the biomechanics of certain cases.

Trunk mass distribution data

A convenience sample of 19 adult male volunteers without known spinal pathology was recruited (10 healthy weight, 9 with obesity) among students and staff of Khalifa University, Abu Dhabi. Torso mass distribution was estimated using an established pipeline for male trunk body shape prediction, which reported high segmentation accuracy and trunk mass estimation errors below 384 g in a validation study [37]. Fifteen anthropometric measurements with respect to anatomical landmarks (distances and circumferences at specific body sites) were taken. Based on them, trunk shape surface topography was predicted using an established machine learning pipeline. The corresponding volume was then analysed for underlying tissues distribution, using machine learning and a template from the Visible Human Project (VHP) Male, to assume organs and tissues within this volume. Considering different tissue densities, mass distribution along the spine was estimated, and segmental masses and CoM locations (with respect to vertebral body centres) calculated from T1 to L5 levels. This approach has been reported in a previous publication [37].

Musculoskeletal spine model

An established musculoskeletal model of the spine [28, 32, 33, 38] using the AnyBody Modelling System software

(AnyBody Technology A/S, Aalborg, Denmark, version 7.4.0) was used to perform standing and forward flexion (30°) simulations. Model validation has been previously performed against in vivo intradiscal pressure measurements in healthy subjects, showing good agreement with predicted compressive forces [32, 33, 38, 39]. In this model, the pelvis was constrained to the ground and rigidly connected to the sacrum. Thoraco-lumbar intervertebral articulations were modelled as three degrees of freedom joints, and the ribcage was represented as a detailed articulated system. Ribcage elasticity was modelled with passive stiffness elements from ex-vivo measurements [40, 41], and intra-abdominal pressure model was included in the lumbar region [42, 43]. Effects of thoracic and lumbar spine ligaments and facet joints were incorporated into segmental stiffness definition [43, 44]. Tendon properties and muscle force-length/velocity relations were not considered. Passive properties of intervertebral discs and ligaments were modelled using elastic elements, neglecting rate-dependent damping. Segmental kinematics were defined as constant ratios of regional motion, according to joint mobility for thoracic [45] and lumbar segments [46]. Weight contributions of upper extremities were considered as forces applied to upper thoracic segments.

The model represented patient-specific alignment and trunk mass distribution from radiographic and anthropometric input data. Positions and orientations of individual thoracic and lumbar vertebrae (T1-L5) were based on vertebral endplate coordinates from the ESSG dataset. Vertebral centroids (centres of four endplate landmarks) and orientations (average inclination of endplates), together with pelvic incidence angle and sacral orientation, were used to model patient-specific sagittal thoraco-lumbar spinopelvic alignment profiles. Cervical spine curvature was adjusted to achieve horizontal gaze. Trunk mass distribution was modelled using segmental masses from T1 to L5 and antero-posterior CoM offset relative to vertebral centroids [37]. Personalized principal components of the inertia tensors (Jx, Jy, Jz) were implemented at each spinal level from linear relationship with segmental masses ($R^2 > 0.98$), established on experimental data from Pearsall et al. [31] (Online Resource 1, Fig. 4).

Synthetic cohorts

Based on available data and study purposes, two synthetic cohorts were created: healthy weight and with obesity. Every sagittal alignment ($N=754$) was considered for each of the available mass distributions ($N=19$) resulting in a dataset representing a full systematic combination of the two parameter sets (Fig. 1). Vertebral centroids coordinates were provided as % of patient's body height (BH), segmental masses and principal components of the inertia tensor as % of volunteer's BM, and CoM locations as % of volunteer's BH. This allowed analysis of isolated effects of alignments and body shape, independently from patients and volunteers BSPs. Due to the method's limitation in predicting mass distribution from T1 to L5, mass redistribution across the trunk, head, pelvis, legs, and arms was applied. The body parameters of the synthetic cohorts were set to BH = 1.80 m for both, with BM=75 kg for the healthy weight group and BM = 100 kg for the obesity group.

Inverse dynamics simulations

For each model representing a combination of sagittal alignment and trunk mass distributions, trunk CoM was calculated as A-P distance from sacral endplate posterior landmark and inverse dynamics simulations were performed to predict spinal loads (Fig. 2). Loads were estimated during

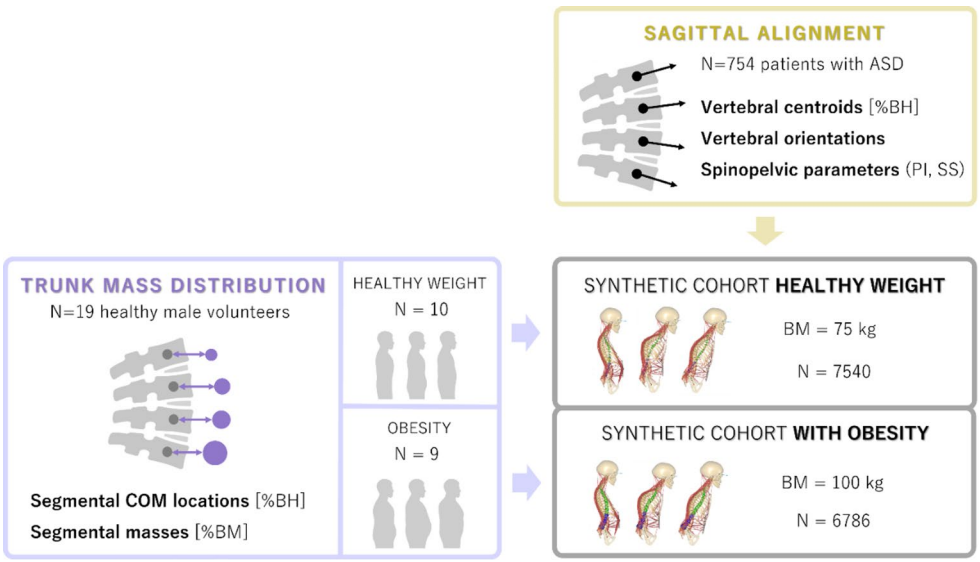

Fig. 1 Synthetic cohorts' design: sagittal alignments of 754 patients with ASD (PI: pelvic incidence, SS: Sacral slope) were assumed for each of the available measures of body mass distribution (10 of healthy weight and 9 with obesity) to create MSK models of two synthetic patient cohorts (healthy weight and with obesity)

static upright-posture and dynamic task of 30° forward flexion, simulated with duration of 50s (quasi-static, flexed posture), 5s (dynamic, slow motion), and 1.5s (dynamic, fast**).** Forward flexion was prescribed as a sagittal-plane motion with a sigmoidal time pattern. The resulting velocity and acceleration profiles corresponding to different motion rates affect dynamic simulations through inertial and velocity-dependent terms of equations of motion. Motion was distributed between spinal regions with a lumbo-pelvic ratio equal to 2 [47] and a thoraco-lumbar ratio of 0.25 [48, 49], and between individual spinal segments, assuming constant ratios based on reported experimental data [50, 51]. This led to a total simulation of 754 alignment profiles x 19 mass distribution patterns x 4 kinematic conditions.

Inverse dynamics approach solves the equations of motion for each segment, based on the force and moment equilibrium requirement. From the loads that are known, it estimates unknown internal forces: muscle forces needed to empower the prescribed motion and posture, and the resulting intervertebral joint reaction forces [52]. Because of muscle redundancy, a muscle optimisation scheme was applied to mimic physiological recruitment of muscles, favouring stronger muscles and muscle synergy while reducing energy expenditure [53]. Polynomial muscle recruitment criterion minimised the sum of squared muscle activities (i.e. ratio of generated muscle force to its strength, or maximum voluntary force) [53]. Predicted loads were normalised to BM.

Statistical analysis

Descriptive analysis

Demographic and body parameters data are presented as mean μ ± standard deviation σ. The Bonferroni-Holm correction for multiple comparisons was applied [54]. Statistical significance was set at $p < 0.05$, with levels indicated as follows: * $p < 0.05$, ** $p < 0.01$, *** $p < 0.001$.

Factorial analysis with generalised linear models

A factorial analysis using generalised linear models (GLMs) assessed the relative effects of sagittal alignment and body shape (predictors) on trunk CoM location and spinal load (responses). Since MSK model outputs are deterministic, random effects accounted for only a negligible portion of the variance in the biomechanical outputs. Therefore, GLMs were used for the factorial analysis. Individual GLMs were implemented for each spinal level (T1-L5) and cohort (healthy weight and with obesity). For a given spinal level, i, the GLM predicted the expected value of each

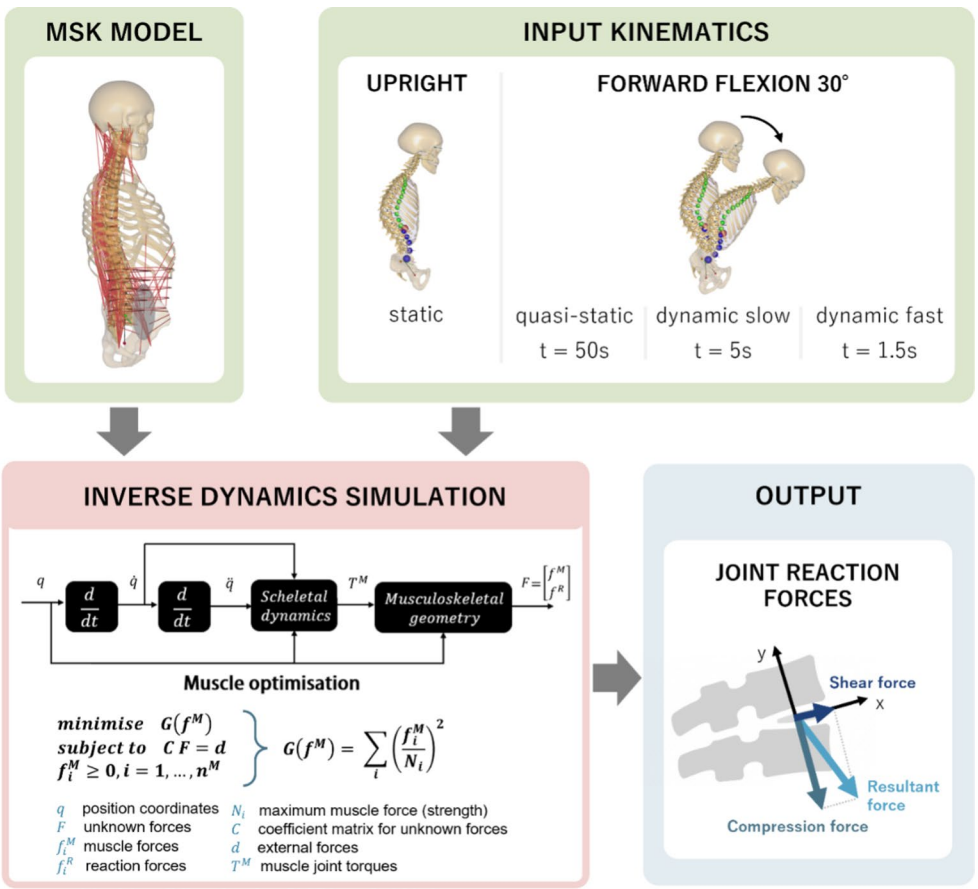

Fig. 2 MSK simulation workflow. For each combination of sagittal alignment and trunk mass distribution profile, musculoskeletal models were created. Inverse dynamics simulations of upright and forward-flexed posture as well as slow and fast dynamic flexion tasks were performed to analyse spinal segmental joint reaction forces (intervertebral spinal loads). Axial compression and antero-posterior shear components were calculated with respect to the intervertebral joint reference frame. The models of synthetic patient also served to calculate trunk centre of mass location, for each combination of alignment and body shape (not shown)

response variable, y_i, as a weighted sum of the j predictors, x_{ij}, [55] scaled by parameters, β_j, plus an error term, ϵ_i, in compact matrix notation: $\boldsymbol{Y} = \boldsymbol{X}\boldsymbol{\beta} + \boldsymbol{\epsilon}$ [56]. The significance of predictors, x_{ij}, was evaluated by testing β_j against zero [57], and F-values were computed to assess each factor's contribution to response variability. The relative effect of each predictor was quantified as the proportion of variance (VP_{ij}, as %) explained by each factor, calculated as factor-specific F-value divided by the sum of the F-values of both predictors.

Estimation of error due to disregarded factor

Error (e) from omitting factor j (mass distribution or sagittal alignment) in spinal load prediction at spinal level i was computed as: $e_{ij} = \sqrt{\frac{VP_{ij}}{100}}\ \sigma_i$ (σ_i, standard deviation of spinal loads across all alignment-shape combinations). This formulation provides a factor-specific estimate of the expected prediction error when a given factor is disregarded. Errors were expressed in N/kg and as % of the mean spinal load. The coefficient of variation quantified the overall variability of gravitational moments and CoM coordinates at spinal levels [58]. Analyses were performed using MATLAB (MATLAB R2022b, v. 9.13.0, MathWorks, Inc.) and SPSS (IBM Corp., Version 28.0. Armonk, NY).

Results

ASD study sample

In the study sample of 754 patients with ASD (Age = 53.0 ± 21.0 years, BM = 63.7 ± 12.5 kg, BMI = 23.9 ± 4.4 kg/m^2) whose sagittal alignment data were used as input for the synthetic cohorts, the majority (n = 615, 81.6%) were women. Eighty-three patients (11%) showed obesity, with 61 of these (73.4%) being female. Regarding deformity representation (Online Resources, Table 1), 394 (52.3%) patients had sagittal malalignment (fulfilled one of the criteria: SVA ≥ 50 mm, PT ≥ 25° or TK ≥ 60°), out of which 318 had also coronal deformity (Cobb angle ≥ 20°), whereas coronal deformity without sagittal malalignment was seen in 360 cases (47.7%). This corresponded to the following sagittal profile representation in the sample, based on GAP classification: 29.4% were proportioned (GAP score 0–2), 32.8% moderately disproportioned (GAP score 3–6), and 37.8% severely disproportioned (GAP score ≥ 7; Online Resources, Table 2). On average (±σ), the sample was characterized by SVA = 26.16 ± 55.37 mm, TK = 38.74 ± 19.72°, PT = 19.34 ± 11.48°, and main curve Cobb angle = 49.23 ± 22.00°.

Mass distribution study sample

The sample of volunteers without known spinal deformity, whose body shape data were used to generate synthetic cohorts, included n = 19 young males, enrolled in two groups, based on BMI threshold: healthy weight, BMI < 30 kg/m² (n = 10, Age = 35.3 ± 8.5 years, BM = 77.2 ± 8.6 kg, BMI = 24.0 ± 1.5 kg/m^2) and with obesity, BMI ≥ 30 kg/m² (n = 9, Age = 33.3 ± 9.8 years, BM = 100.0 ± 8.6 kg, BMI = 32.1 ± 2.3 kg/m^2). The healthy-weight group included both normal-weight (n = 7, BMI < 25 kg/m²) and mildly overweight subjects (n = 3, BMI ≥ 25 kg/m²), while the obesity group included volunteers with both Class I (n = 7) and Class II obesity (n = 2, BMI ≥ 35 kg/ m²), with maximum BMI = 35.9 kg/m². Fraction of body mass %BM carried by individual spinal segments was significantly greater in subjects with obesity compared to healthy weight, and greater variability was observed in the healthy weight group (Fig. 3, left). A-P position of segmental CoM (normalised to BH) was slightly greater (more anterior) in subjects with obesity for most thoracic and all lumbar segments (Fig. 3, right) and showed greater variability in middle/lower thoracic segments (Online Resources, Fig. 2).

Relative effect of spinal alignment and body shape on trunk centre of mass location

A-P location of trunk CoM measured from the sacral endplate posterior landmark was found to be primarily determined by sagittal alignment in both healthy weight and obese cohorts, with relative effects 96% and 89%, respectively. In other words, the influence of mass distribution was comparatively small, although greater in the cohort with obesity than in the healthy-weight (11% vs. 4%). Vertical position of the trunk CoM in the healthy weight cohort was mainly driven by mass distribution (relative effect 93%), whereas in the group with obesity, mass distribution and alignment contributed at a ratio of 54%:46%.

Relative effect of spinal alignment and body shape on spinal loads

In the simulated healthy weight cohort, compressive loads were affected by trunk mass distribution with greatest effects in the lower lumbar region (42–57%, max at L5-Sacrum level) and in the upper thorax (14–98%, max at T1-T2) (Fig. 4). In the obese cohort, mass distribution and sagittal alignment exerted comparable influence on spinal compressive forces, the former predominating in thoracic levels (24–98%, max T1-T2) and the latter in the lumbar (73–81%, max at L3-L4). Shear forces were mainly determined by

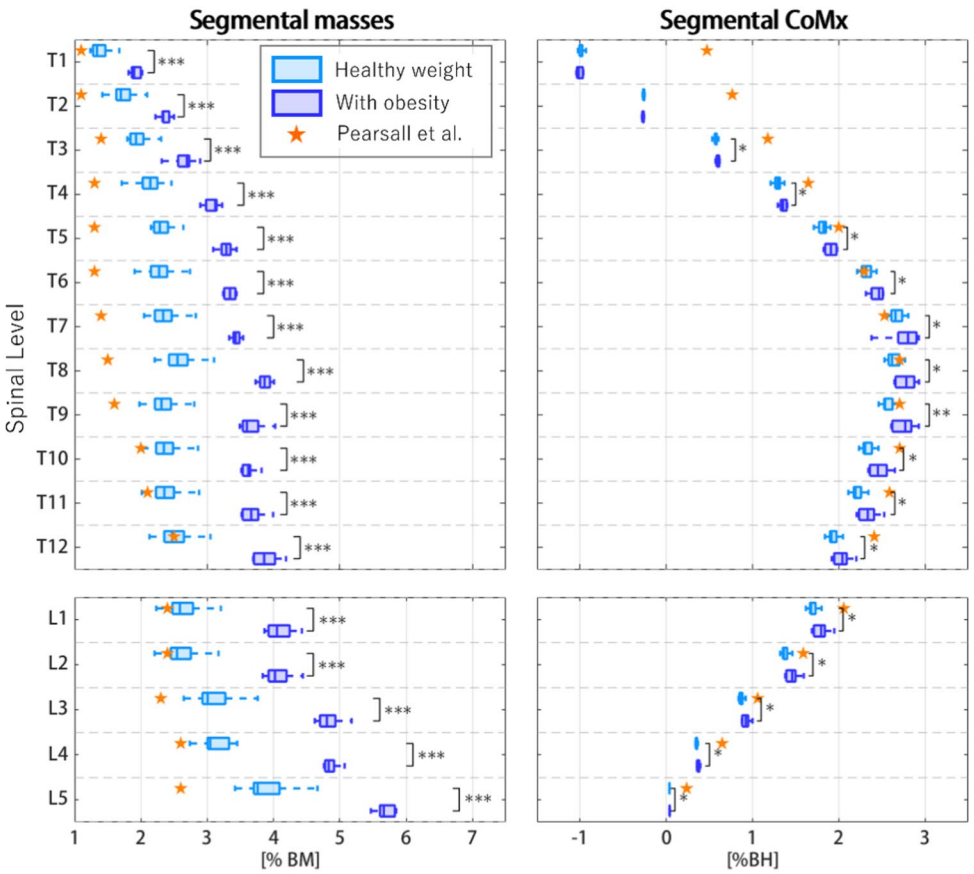

Fig. 3 Body shape parameters: masses associated with spinal segments and antero-posterior positions of segmental CoM, estimated for 19 male volunteers, based on measured anthropometric data and modelling of body volume and tissue composition [37]. For reference, data derived from CT scans of 6 subjects reported in Pearsall et al. [31] are also presented. The asterisks denote statistically significant differences between healthy and with obesity subjects, with *: $p < 0.05$, **: $p < 0.01$, and ***: $p < 0.001$

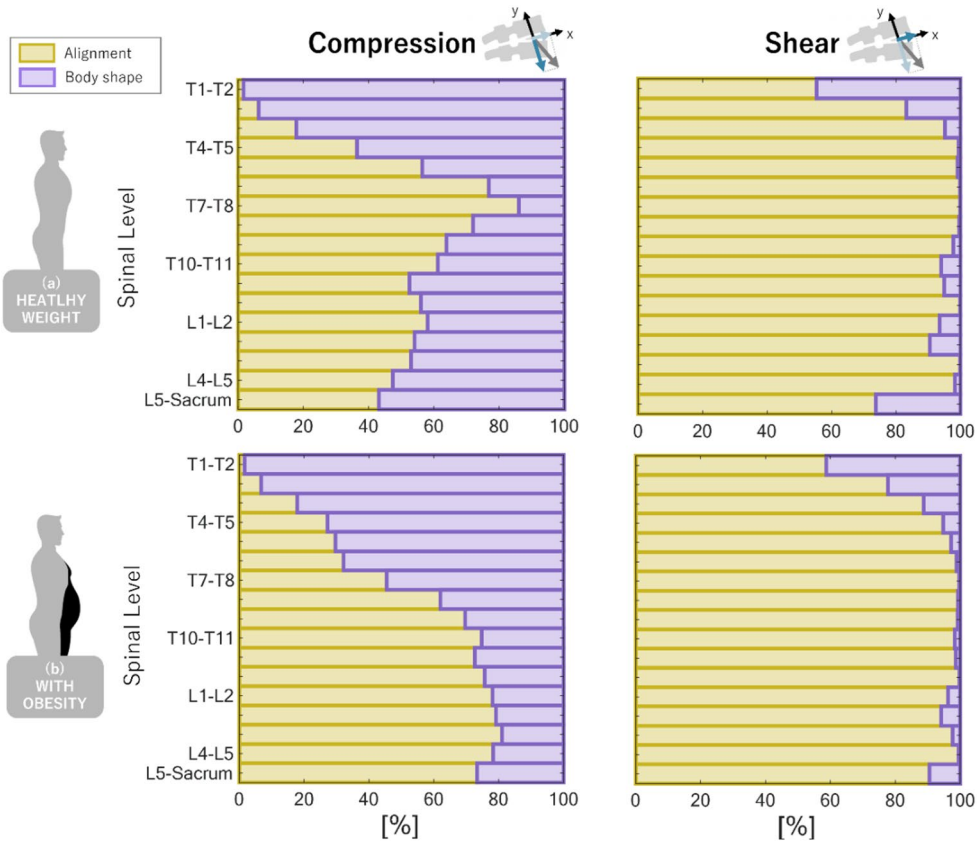

Fig. 4 Relative effect of sagittal alignment (yellow) and mass distribution (purple) on compressive (left) and shear (right) joint reaction forces in healthy weight (**a**) and obese (**b**) cohorts during static standing

sagittal alignment in both cohorts, with relative effects ranging 55%-100% (max at T12-L1) in the healthy weight, and 57%-100% (max at T12-L1 level) in the obesity group.

During the fast dynamic forward flexion task, body mass distribution effect on compressive forces was within similar range to and showing similar trends between segments as during standing (Fig. 5). Instead, it had substantial influence on thoracic shear forces, up to 91% and 92% of relative effect in healthy weight and obese cohorts, respectively. Similar findings were found across the simulated conditions of quasi-static, dynamic slow and dynamic fast flexion tasks (Online Resource 1, Fig. 3).

Errors in spinal loads due to mass distribution and alignment

The largest prediction error associated with disregarding mass distribution during standing was found at L4-L5 and L5-Sacrum spinal levels, with errors in the healthy weight cohort reaching ± 2.5 N/kg (± 20.3% of μ) and in the obese cohort, ± 1.7 N/Kg (± 13.3% of μ) at same spinal levels (Fig. 6).

Discussion

Understanding biomechanical factors driving spinal loading in sagittal deformities is central for improving clinical outcomes. Musculoskeletal (MSK) studies have shown that body mass (BM) [29, 30] and body shape parameters (BSPs) [34], as well as pathological [59, 60] and surgically corrected [28] spinal curvatures, influence loading patterns. Although recent models have incorporated subject-specific mass distributions and spinal alignments [35, 36], their relative biomechanical contributions remain unclear. This study quantifies the impact of alignment and body shape on trunk CoM location and intervertebral reaction forces in synthetic cohorts of patients with ASD during standing and forward flexion, and evaluates load prediction errors when body shape is ignored.

Consistent with studies emphasising sagittal balance as key driver of ergonomic posture [7, 61, 62], we demonstrated that spinal alignment exerts a dominant effect on the A-P location of trunk CoM, whereas body shape contributes to it comparatively little. This finding reinforces the biomechanical relevance of surgical realignment of sagittal curvatures to reposition the CoM within the "cone of efficiency", even in obese patients, where central adiposity shifts trunk segment CoM anteriorly [63, 64], congruent with current alignment-based surgical planning strategies [65]. Along the cranio-caudal axis on the other hand, the trunk CoM location was primarily determined by body shape. Vertical variability in body mass distribution modulates the load transfer along the spine: increased upper-trunk mass raises the CoM (as in gymnasts [66]), whereas lower-trunk accumulation shifts it downward (e.g., in elderly women [67] and individuals with obesity [63]). Because alignment had only a mild impact on vertical CoM location, effective load management across the spine should also consider thoracic vs. lumbar body proportions variability, particularly if patient-specific loading is to be incorporated into surgical planning in the future.

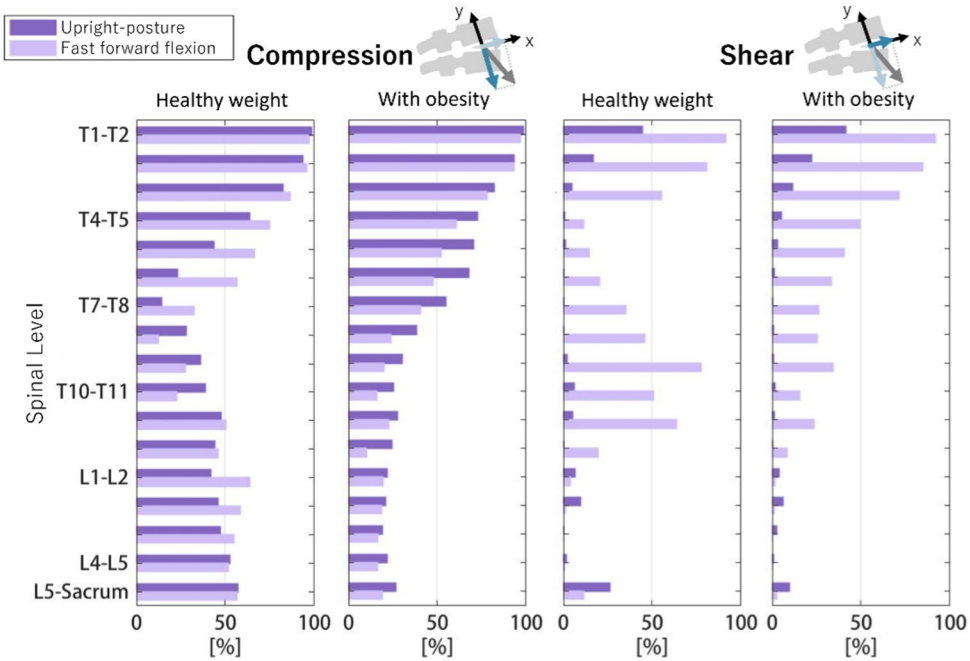

Fig. 5 Relative effect of mass distribution on spinal loads during fast dynamic 30° forward flexion simulations (faint purple) compared to static upright-posture (dark purple). Sagittal alignment effects (not shown) are the complement to 100%

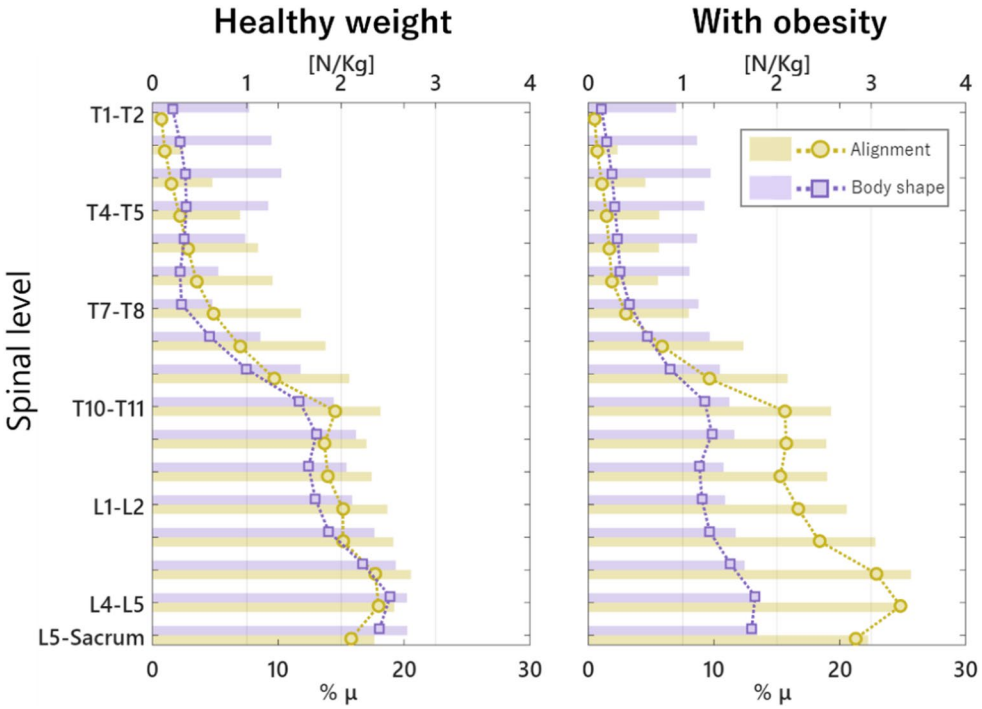

Fig. 6 Prediction error in compressive loads associated with sagittal alignment (yellow) and mass distribution (purple), expressed in absolute values of force per kg of body mass (symbol markers on upper x-axis) and in relation to the cohort's overall variability (bars on lower x-axis)

Consistently with vertical position of CoM, model-predicted spinal segmental loads were also profoundly affected by body shape, in both standing and forward bending tasks. In static simulations, larger variability in gravitational moments rendered compression loads more sensitive to mass distribution in the healthy weight than in the obesity group. Ignoring body shape caused similar substantial errors in estimated axial loads at L4-L5 and L5-Sacrum (± 20% in healthy weight, ± 13% in obese), clinically relevant levels prone to disc degeneration [68], associated with low back pain [69]. These results suggest that incorporating subject-specific mass distribution, as previously done in healthy MSK models [35, 36], is essential when modelling not only spinal deformities but also other pathologies for the accuracy of load predictions. Sagittal alignment was found to be a primary driver of shear forces during posture maintenance, a result not surprising, as vertebral orientation dictates load projection on vertebral endplates. Spinal malalignments exacerbate A-P shear [28, 70], clinically linked to spine pathologies [71], in particular spondylolisthesis [72] and shear-related lumbar injury risk [73]. On the other hand, forward flexion revealed that mass distribution influenced thoracic shear more than alignment by modifying gravitational leverage from trunk inclination [74].

ASD correction planning based solely on static alignment metrics (Schwab modifiers [7], Lafage formula [75] and Global Alignment Proportion (GAP) score [76]) targets restoring sagittal profile, which might not guarantee optimal postoperative biomechanics, neither in standing nor in motion. Our study demonstrates both are likely affected by body shape, which might contribute to segment-specific mechanical overload. For instance, considering body shape information could guide selection of upper instrumented vertebrae to avoid excessive stress at proximal segment or could help predicting and preventing excessive loads on the construct. Notably, shear load variations observed in thoracic regions during forward bending may intensify stress, increasing risk of proximal junctional kyphosis (PJK) and failure (PJF). Patients who receive thoracic fusion may experience higher adjacent-segment loads if they show more body mass accumulated in chest region, compared to patients with pear-like body shape, which might be particularly relevant for planning ASD surgery in females.

Studies on PJK/PJF risk assessment have focused on global sagittal alignment [10, 77, 78], spinal loads [28], musculature [79–81], instrumentation effects [82–85] and BMI [86]. Although direct impact of body shape on PJK/PJF has not been explored, our finding suggests it could be relevant. Given higher complication rates in obese patients undergoing ASD corrective surgery [11], and the substantial effect of body shape on spine biomechanics demonstrated in this study, preoperative weight management as well as surgical planning informed by body shape could optimize biomechanical and clinical outcomes. Post-surgery, counselling at risk patients to minimize deep forward flexion maneuvers, or adopting modified techniques, could be envisioned to reduce excessive loads exposure at vulnerable spinal segments. Similarly, in conservative care, physiotherapists could tailor exercises and promote daily movement strategies emphasizing safe bending forward or lifting,

but more research is needed to determine effectiveness of such interventions. In particular, longitudinal follow-up of ASD patients integrating body shape measurement with alignment changes into subject-specific MSK and FE models [87] in the future will explore how predicted differences in loads due to alignment vs. mass distribution translate into mechanical complications. Although this study was not designed to test the influence of various surgical strategies or predict patient-specific postoperative complications, the findings highlight the potential value of integrating body shape into planning of ASD correction, bridging the gap between alignment-based correction and biomechanical optimization. Future work should include analyses of postoperative alignments in the context of complication outcomes to assess how body shape might influence complication risk after ASD correction.

This study had the following limitations:

1. Mass distribution data was based on 19 young male subjects without known spinal pathology from the UAE, limiting variability in simulated body shapes and generalizability. Body shape varies with age [88] and sex [89], potentially affecting spinal biomechanics. Because interactions between spinal alignment and body shape are also expected [90, 91], future studies should collect larger and more representative body shape datasets for patients with ASD, including older individuals and females, to confirm the study findings and better represent the real patient population. Nonetheless, the substantial impact of even this restricted body shape variability on spine biomechanics indicates that inclusion of a broader dataset would likely amplify the observed effects. Ideally, future analyses should include patient-specific BSPs, and imaging-based approaches (e.g., bi-planar slot scanner [35]), neural network reconstructions combined with anthropometry [37], or 3D scanners [15], could provide tools for their estimation. Right clinical parameters to sufficiently describe mass distribution remain to be identified. Simplified descriptors, such as global or regional centre of mass location, or a classification of body shape types, are desirable from a practical standpoint; however, their ability to capture the biomechanical effects observed in this study must be evaluated in future work.
2. A single set of tissue densities was used to calculate CoM and segmental masses, regardless of weight category [37]. Adopting CT scans of obese subjects could provide even more accurate BSPs estimation.
3. MSK model only represented sagittal deformities, disregarding coronal misalignments. In 3D deformities, body shape would affect lateral shear forces, as trunk CoM shifts along medio-lateral axis based on scoliotic curvature, increasing mechanical demands.
4. The alignment of cervical vertebrae was assumed in the model due to missing radiographic annotations. The model's cervical spine was adjusted to maintain a horizontal gaze, replicating compensatory mechanisms [92]. Despite this, load transmission may be affected with cascading effects.
5. The musculoskeletal model has been previously validated for selected postures and spinal levels in healthy subjects [32, 33]. Direct validation in patients with ASD remains challenging due to the invasiveness and limited availability of in vivo data [93]; nevertheless, efforts should be made in the future to validate such models for use in patient cohorts.
6. Forward flexion was prescribed using a simplified sagittal-plane motion rather than subject-specific motion capture data. Potential differences in segmental coordination, as well as out-of-plane movements, were not represented. Future studies incorporating motion capture data could provide a subject-specific description of movement and allow the analysis of additional daily living motion tasks, e.g. sitting transitions relevant for ASD [94, 95]. Spinal alignment modelling should also be expanded beyond upright standing to sitting postures in the future, to capture effects of spinal alignment perhaps more representative of daily habits.
7. Segmental analyses were based on fixed anatomical levels (e.g., T7, T12). However, due to variability in pelvic incidence and sagittal alignment (e.g., Roussouly types), these levels do not consistently map to the same functional regions (e.g., thoracic apex or thoracolumbar junction), limiting clinical interpretation.

Conclusion

This study demonstrates the impact of body shape on adult spinal deformity biomechanics. While it does not seem to substantially influence overall sagittal balance (trunk centre of mass), it should be confirmed in future analyses of patient-specific (age, sex, body mass index) body shapes. Nevertheless, the profound effect of body shape on spinal loads suggests that thoracic and lumbar mass distribution should be considered in future research as complementary biomechanical parameters in ASD surgical planning to avoid mechanical overloading of instrumentation or spinal segments prone to proximal junction complications.

Supplementary Information The online version contains supplementary material available at https://doi.org/10.1007/s00586-026-10243-5.

Acknowledgements We acknowledge the invaluable contribution of the Statistical Office of ETH Zurich. We are grateful to Graz Lukas for his guidance on the statistical methodology. This project was

conducted as a Master's thesis supported by the "Thesis Abroad" scholarship from Politecnico di Milano.

Author contributions Conceptualization: ER, MER, ML, FG, SJF, DI. Methodology: ER, DI. Software: ER, AH, TL, DI. Validation: ER, DI. Formal analysis: ER. Investigation: ER. Resources: AH, TL, MER, ML, FK, TF, DH, SRW, FP, IO, JP, AA, CY, SJF, DI. Data curation: ER. Writing - original draft preparation: ER. Writing - review and editing: ER, AH, TL, MER, ML, FG, FK, TF, DH, SRW, FP, IO, JP, AA, CY, LLB, SJF, DI. Visualization: ER, DI. Supervision: ML, FG, LLB, SJF, DI. Project administration: ER, DI. Funding acquisition: ER, LLB.

Funding Open access funding provided by Swiss Federal Institute of Technology Zurich

Data availability The data used in this study are not publicly available. Further details on data sources are provided in the Methods section. Derived data supporting the findings of this study are available from the corresponding author upon reasonable request.

Declarations

Competing interests The authors declare no competing interests.

Open Access This article is licensed under a Creative Commons Attribution 4.0 International License, which permits use, sharing, adaptation, distribution and reproduction in any medium or format, as long as you give appropriate credit to the original author(s) and the source, provide a link to the Creative Commons licence, and indicate if changes were made. The images or other third party material in this article are included in the article's Creative Commons licence, unless indicated otherwise in a credit line to the material. If material is not included in the article's Creative Commons licence and your intended use is not permitted by statutory regulation or exceeds the permitted use, you will need to obtain permission directly from the copyright holder. To view a copy of this licence, visit http://creativecommons.org/licenses/by/4.0/.

References

1. Cerpa M, Lenke LG, Fehlings MG, Shaffrey CI, Cheung KMC, Carreon LY (2019) Evolution and Advancement of Adult Spinal Deformity Research and Clinical Care: An Overview of the Scoli-RISK-1 Study. Global Spine J 9(1_suppl,):8S-14S. https://doi.org/10.1177/2192568219828729
2. Le Huec J-C, Thompson W, Mohsinaly Y, Barrey C, Faundez A (2019) Sagittal balance of the spine. Eur Spine J 28:1889–1905
3. Diebo BG et al (2019) Adult spinal deformity. Lancet 394(10193):160–172
4. Totera JIC, Valenzuela JGF, Arancibia JAG, Contreras STP, Lalanne LB, Alvarez-Lemos FL (2021) Sagittal balance: from theory to clinical practice. EFORT Open Rev 6(12):1193–1202
5. Glassman SD, Berven S, Bridwell K, Horton W, Dimar JR (2005) Correlation of radiographic parameters and clinical symptoms in adult scoliosis. Spine (Phila Pa (1976)) 30(6):682–688
6. Pellisé F et al (2015) Impact on health related quality of life of adult spinal deformity (ASD) compared with other chronic conditions. Eur Spine J 24:3–11
7. Schwab F, Patel A, Ungar B, Farcy J-P, Lafage V (2010) Adult spinal deformity—postoperative standing imbalance: how much can you tolerate? An overview of key parameters in assessing alignment and planning corrective surgery. Spine (Phila Pa (1976)) 35(25):2224–2231
8. Dubousset J (1994) Three-dimensional analysis of the scoliotic deformity. In: Weinstein SL (ed) Pediatric Spine: Principles and Practice, 1st edn. Raven, New York, pp 479–483.
9. Celestre PC, Dimar JR, Glassman SD (2018) Spinopelvic Parameters: Lumbar Lordosis, Pelvic Incidence, Pelvic Tilt, and Sacral Slope: What Does a Spine Surgeon Need to Know to Plan a Lumbar Deformity Correction? Neurosurg. Clin N Am 29(3):323–329. https://doi.org/10.1016/j.nec.2018.03.003
10. Cho M, Lee S, Kim HJ (2024) Assessing the predictive power of the GAP score on mechanical complications: a comprehensive systematic review and meta-analysis. Eur Spine J 33(4):1311–1319. https://doi.org/10.1007/s00586-024-08135-7
11. Soroceanu A et al (2015) Impact of obesity on complications, infection, and patient-reported outcomes in adult spinal deformity surgery. J Neurosurg Spine 23(5):656–664
12. Organization WH (1995) Physical status: The use of and interpretation of anthropometry, Report of a WHO Expert Committee. World Health Organization
13. Jackson KL, Devine JG (2016) The effects of obesity on spine surgery: A systematic review of the literature. Global Spine J 6(4):394–400. https://doi.org/10.1055/s-0035-1570750
14. Hammer A et al (2025) Early revision rate after posterior spinal fusion surgery increases with every additional BMI point. Eur Spine J 34(5):1943–1953. https://doi.org/10.1007/s00586-025-08726-y
15. Faust ME, Carrier S (2011) 3D body scanning: Generation Y body perception and virtual visualization, Computer Technology for Textiles and Apparel, pp. 219–244. https://doi.org/10.1533/9780857093608.3.219
16. Nakamura K, Kurokawa T (2009) Analysis and classification of three-dimensional trunk shape of women by using the human body shape model. Int J Comput Appl Technol 34(4):278–284. https://doi.org/10.1504/IJCAT.2009.024080
17. Vegas L, Wilson A, Istook C (2019) Body Shape Classifications of Males 26 to 35 Using Size USA Three-Dimensional Scan Data, Int. Textile Apparel Assoc. Annu. Conf. Proc., 76(1). https://doi.org/10.31274/itaa.8805
18. Ben Azouz Z, Rioux M, Shu C, Lepage R (2006) Characterizing human shape variation using 3D anthropometric data. Visual Comput 22(5):302–314. https://doi.org/10.1007/S00371-006-0006-6/METRICS
19. Harrison CR, Robinette KM (2002) CAESAR: Summary statistics for the adult population (ages 18–65) of the United States of America. Air Force Research Laboratory, Human Effectiveness Directorate, Crew System, AFB, OH, USA, Wright-Patterson
20. Consultation WE (2008) Waist circumference and waist-hip ratio, Report of a WHO Expert Consultation. World Health Organization, Geneva, pp 8–11
21. Veitch D, Robinette K (2006) World Engineering Anthropometry Resource (WEAR): A Review, in Human Factors and Ergonomics Society of Australia Inc. Annual Conference
22. Zakaria N (2017) Evaluation of fit and size, Manikins for Textile Evaluation. 89–113. https://doi.org/10.1016/B978-0-08-100909-3.00004-2
23. Reed MP, Raschke U, Tirumali R, Parkinson MB (2014) Developing and implementing parametric human body shape models in ergonomics software, in ASME Design Engineering Technical Conference
24. Reed MP, Parkinson MB (2008) Modeling Variability in Torso Shape for Chair and Seat Design, Proceedings of the ASME Design Engineering Technical Conference, 1(Parts a and B):561–569. https://doi.org/10.1115/DETC2008-49483
25. Ng BK et al (2019) Detailed 3-dimensional body shape features predict body composition, blood metabolites, and functional

strength: the Shape Up! studies. Am J Clin Nutr 110(6):1316–1326. https://doi.org/10.1093/AJCN/NQZ218
26. Senteler M, Weisse B, Rothenfluh DA, Farshad MT, Snedeker JG (2017) Fusion angle affects intervertebral adjacent spinal segment joint forces—Model-based analysis of patient specific alignment. J Orthop Res 35(1):131–139. https://doi.org/10.1002/JOR.23357
27. Ignasiak D, Peteler T, Fekete TF, Haschtmann D, Ferguson SJ (2018) The influence of spinal fusion length on proximal junction biomechanics: a parametric computational study. Eur Spine J 27(9):2262–2271. https://doi.org/10.1007/S00586-018-5700-3
28. Ignasiak D et al (2023) Association between sagittal alignment and loads at the adjacent segment in the fused spine: a combined clinical and musculoskeletal modeling study of 205 patients with adult spinal deformity. Eur Spine J 32(2):571–583
29. Han K-S, Rohlmann A, Zander T, Taylor WR (2013) Lumbar spinal loads vary with body height and weight. Med Eng Phys 35(7):969–977
30. Ghezelbash F, Shirazi-Adl A, Arjmand N, El-Ouaaid Z, Plamondon A, Meakin JR (2016) Effects of sex, age, body height and body weight on spinal loads: Sensitivity analyses in a subject-specific trunk musculoskeletal model. J Biomech 49(14):3492–3501
31. Pearsall DJ, Reid JG, Livingston LA (1996) Segmental inertial parameters of the human trunk as determined from computed tomography. Ann Biomed Eng 24:198–210
32. Ignasiak D, Ferguson SJ, Arjmand N (2016) A rigid thorax assumption affects model loading predictions at the upper but not lower lumbar levels. J Biomech 49(13):3074–3078
33. Ignasiak D, Dendorfer S, Ferguson SJ (2016) Thoracolumbar spine model with articulated ribcage for the prediction of dynamic spinal loading. J Biomech 49(6):959–966
34. Liu T, Hulleck AA, El-Rich M (2023) Sensitivity of subject-specific upper body musculoskeletal model predictions to mass scaling methods. Comput Biol Med 165:107376
35. Fasser Marie-Rosa KM, Moritz J, Gomez Romero DA, Tudor T, Snedeker JG, Farshad M, Jonas W (2021) Subject-specific alignment and mass distribution in musculoskeletal models of the lumbar spine. Front Bioeng Biotechnol 9:721042
36. Lerchl T et al (2022) Validation of a patient-specific musculoskeletal model for lumbar load estimation generated by an automated pipeline from whole body CT. Front Bioeng Biotechnol 10:862804
37. Liu T, Khalaf K, Hebela N, Westover L, Galbusera F, El-Rich M (2021) Prediction of human male trunk mass distribution using anthropometric measurements: A feasibility study. J Biomech 122:110437
38. De Zee M, Hansen L, Wong C, Rasmussen J, Simonsen EB (2007) A generic detailed rigid-body lumbar spine model. J Biomech 40(6):1219–1227
39. Bassani T, Stucovitz E, Qian Z, Briguglio M, Galbusera F (2017) Validation of the AnyBody full body musculoskeletal model in computing lumbar spine loads at L4L5 level. J Biomech 58:89–96. https://doi.org/10.1016/j.jbiomech.2017.04.025
40. Andriacchi T, Schultz A, Belytschko T, Galante J (1974) A model for studies of mechanical interactions between the human spine and rib cage. J Biomech 7(6):497–507
41. Schultz AB, Benson DR, Hirsch C (1974) Force-deformation properties of human costo-sternal and costo-vertebral articulations. J Biomech 7(3):311–318
42. Arshad R, Zander T, Dreischarf M, Schmidt H (2016) Influence of lumbar spine rhythms and intra-abdominal pressure on spinal loads and trunk muscle forces during upper body inclination. Med Eng Phys 38(4):333–338
43. Han K-S, Zander T, Taylor WR, Rohlmann A (2012) An enhanced and validated generic thoraco-lumbar spine model for prediction of muscle forces. Med Eng Phys 34(6):709–716
44. Schmidt TA, An HS, Lim T-H, Nowicki BH, Haughton VM (1998) The stiffness of lumbar spinal motion segments with a high-intensity zone in the anulus fibrosus, Spine (Phila. Pa. (1976))., 23(20):2167–2173
45. Boos N, Aebi M (eds) (2008) Spinal Disorders: Fundamentals of Diagnosis and Treatment, 1st edn. Springer. https://doi.org/10.1007/978-3-540-69091-7
46. Arjmand N, Shirazi-Adl A (2006) Model and in vivo studies on human trunk load partitioning and stability in isometric forward flexions. J Biomech 39(3):510–521
47. Esola MA, McClure PW, Fitzgerald GK, Siegler S (1996) Analysis of lumbar spine and hip motion during forward bending in subjects with and without a history of low back pain, Spine (Phila. Pa. (1976))., 21(1):71–78
48. Arshad R, Pan F, Reitmaier S, Schmidt H (2019) Effect of age and sex on lumbar lordosis and the range of motion. A systematic review and meta-analysis. J Biomech 82:1–19. https://doi.org/10.1016/j.jbiomech.2018.11.022
49. Pan F, Firouzabadi A, Reitmaier S, Zander T, Schmidt H (2018) The shape and mobility of the thoracic spine in asymptomatic adults – A systematic review of in vivo studies. J Biomech 78:21–35. https://doi.org/10.1016/j.jbiomech.2018.07.041
50. Wilke HJ, Herkommer A, Werner K, Liebsch C (2017) In vitro analysis of the segmental flexibility of the thoracic spine. PLoS ONE 12(5). https://doi.org/10.1371/journal.pone.0177823
51. Wong KWN, Leong JCY, Chan M, Luk KDK, Lu WW (2004) The Flexion–Extension Profile of Lumbar Spine in 100 Healthy Volunteers, Spine (Phila. Pa. (1976))., 29(15), [Online]. Available: https://journals.lww.com/spinejournal/fulltext/2004/08010/the_flexion_extension_profile_of_lumbar_spine_in.11.aspx
52. Erdemir A, McLean S, Herzog W, van den Bogert AJ (2007) Model-based estimation of muscle forces exerted during movements. Clin Biomech Elsevier Ltd 22(2):131–154
53. Rasmussen J, Damsgaard M, Voigt M (2001) Muscle recruitment by the min/max criterion—a comparative numerical study. J Biomech 34(3):409–415
54. Holm S (1979) A Simple Sequentially Rejective Multiple Test Procedure, Scandinavian Journal of Statistics, 6(2):65–70, [Online]. Available: http://www.jstor.org/stable/4615733
55. Dobson AJ, Barnett AG (2018) An introduction to generalized linear models. Chapman and Hall/CRC
56. Monti MM (2011) Statistical analysis of fMRI time-series: A critical review of the GLM approach. Front Hum Neurosci no MARCH. https://doi.org/10.3389/fnhum.2011.00028
57. Madsen H, Thyregod P (2010) Introduction to general and generalized linear models. CRC
58. Abdi H (2010) Coefficient of variation. Encyclopedia Res Des 1(5):169–171
59. Briggs AM et al (2007) Thoracic kyphosis affects spinal loads and trunk muscle force. Phys Ther 87(5):595–607
60. Bruno AG, Anderson DE, D'Agostino J, Bouxsein ML (2012) The effect of thoracic kyphosis and sagittal plane alignment on vertebral compressive loading. J Bone Miner Res 27(10):2144–2151
61. Glassman SD, Bridwell K, Dimar JR, Horton W, Berven S, Schwab F (2005) The impact of positive sagittal balance in adult spinal deformity, Spine (Phila. Pa. (1976))., 30(18):2024–2029
62. Schwab FJ et al (2013) Radiographical spinopelvic parameters and disability in the setting of adult spinal deformity: a prospective multicenter analysis. Spine (Phila Pa. 1976)., 38(13):803–812.
63. Pryce R, Kriellaars D (2014) Body segment inertial parameters and low back load in individuals with central adiposity. J Biomech 47(12):3080–3086. https://doi.org/10.1016/j.jbiomech.2014.06.038
64. Akhavanfar MH, Kazemi H, Eskandari AH, Arjmand N (2018) Obesity and spinal loads; a combined MR imaging and subject-specific modeling investigation. J Biomech 70:102–112

65. Kim HJ et al (2020) Adult spinal deformity: current concepts and decision-making strategies for management. Asian Spine J 14(6):886
66. WS E (2018) Center of mass of the human body helps in analysis of balance and movement. MOJ Appl Bionics Biomech 2(2). https://doi.org/10.15406/mojabb.2018.02.00057
67. Okada H, AE M, Fujii N, Morioka Y (1996) Body segment inertia properties of japanese elderly. Biomechanisms, 13:125–139. https://doi.org/10.3951/biomechanisms.13.125
68. Saleem S, Aslam HM, Rehmani MAK, Raees A, Alvi AA, Ashraf J (2013) Lumbar Disc Degenerative Disease: Disc Degeneration Symptoms and Magnetic Resonance Image Findings. Asian Spine J 7(4):322–334. https://doi.org/10.4184/asj.2013.7.4.322
69. Brinjikji W et al (2015) MRI Findings of Disc Degeneration are More Prevalent in Adults with Low Back Pain than in Asymptomatic Controls: A Systematic Review and Meta-Analysis. Am J Neuroradiol 36(12):2394. https://doi.org/10.3174/ajnr.A4498
70. Roussouly P, Pinheiro-Franco JL (2011) Biomechanical analysis of the spino-pelvic organization and adaptation in pathology. Eur Spine J 20(5):609. https://doi.org/10.1007/s00586-011-1928-x
71. Castelein RM, van Dieën JH, Smit TH (2005) The role of dorsal shear forces in the pathogenesis of adolescent idiopathic scoliosis–a hypothesis. Med Hypotheses 65(3):501–508
72. Troup JDG (1976) Mechanical factors in spondylolisthesis and spondylolysis. Clin Orthop Relat Res (1976–2007) 117:pp59–67
73. Gallagher S, Marras WS (2012) Tolerance of the lumbar spine to shear: a review and recommended exposure limits. Clin Biomech Elsevier Ltd 27(10):973–978
74. Takahashi I, Kikuchi S, Sato K, Sato N (2006) Mechanical load of the lumbar spine during forward bending motion of the trunk–a biomechanical study. Spine (Phila Pa. 1976) 31(1):18–23
75. Smith JS et al (2012) Dynamic changes of the pelvis and spine are key to predicting postoperative sagittal alignment after pedicle subtraction osteotomy: a critical analysis of preoperative planning techniques. Spine (Phila Pa. 1976) 37(10):845–853
76. Yilgor C et al (2017) Global alignment and proportion (GAP) score: development and validation of a new method of analyzing spinopelvic alignment to predict mechanical complications after adult spinal deformity surgery. JBJS 99(19):1661–1672
77. Noh SH et al (2023) Predicting mechanical complications after adult spinal deformity operation using a machine learning based on modified global alignment and proportion scoring with body mass index and bone mineral density. Neurospine 20(1):265
78. Bridwell KH et al (2013) Proximal junctional kyphosis in primary adult deformity surgery: evaluation of 20 degrees as a critical angle. Neurosurgery 72(6):899–906
79. Yuan L, Zeng Y, Chen Z, Li W, Zhang X, Mai S (2021) Degenerative lumbar scoliosis patients with proximal junctional kyphosis have lower muscularity, fatty degeneration at the lumbar area. Eur Spine J 30:1133–1143
80. Hyun S-J, Kim YJ, Rhim S-C (2016) Patients with proximal junctional kyphosis after stopping at thoracolumbar junction have lower muscularity, fatty degeneration at the thoracolumbar area. Spine J 16(9):1095–1101
81. Pennington Z et al (2019) Paraspinal muscle size as an independent risk factor for proximal junctional kyphosis in patients undergoing thoracolumbar fusion: Presented at the 2019 AANS/CNS Joint Section on Disorders of the Spine and Peripheral Nerves. J Neurosurg Spine 31(3):380–388
82. Kim HJ, Yagi M, Nyugen J, Cunningham ME, Boachie-Adjei O (2012) Combined anterior-posterior surgery is the most important risk factor for developing proximal junctional kyphosis in idiopathic scoliosis. Clin Orthop Relat Res 470:1633–1639
83. Doodkorte RJP, Vercoulen TFG, Roth AK, de Bie RA, Willems PC (2021) Instrumentation techniques to prevent proximal junctional kyphosis and proximal junctional failure in adult spinal deformity correction—a systematic review of biomechanical studies. Spine J 21(5):842–854
84. Mummaneni PV et al (2016) Does minimally invasive percutaneous posterior instrumentation reduce risk of proximal junctional kyphosis in adult spinal deformity surgery? A propensity-matched cohort analysis. Neurosurgery 78(1):101–108
85. Maruo K et al (1976) Predictive factors for proximal junctional kyphosis in long fusions to the sacrum in adult spinal deformity. Spine (Phila Pa) 38(23):E1469–E1476
86. Kim JS et al (2019) Surgical, radiographic, and patient-related risk factors for proximal junctional kyphosis: a meta-analysis. Global Spine J 9(1):32–40
87. Nispel K, Lerchl T, Senner V, Kirschke JS (2023) Recent Advances in Coupled MBS and FEM Models of the Spine—A. Rev Bioeng 10(3). https://doi.org/10.3390/bioengineering10030315
88. Wells JCK (2007) Sexual dimorphism of body composition, Best Pract. Res Clin Endocrinol Metab 21(3):415–430. https://doi.org/10.1016/j.beem.2007.04.007
89. Ross R, Shaw KD, Rissanen J, Martel Y, De Guise J, Avruch L (1994) Sex differences in lean and adipose tissue distribution by magnetic resonance imaging: anthropometric relationships. Am J Clin Nutr 59(6):1277–1285. https://doi.org/10.1093/AJCN/59.6.1277
90. Onyemaechi NOC, Anyanwu GE, Obikili EN, Onwuasoigwe O, Nwankwo OE (2016) Impact of overweight and obesity on the musculoskeletal system using lumbosacral angles. Patient Prefer Adherence, 10:291–296
91. Qi H et al (2024) Association of Body Mass Index and Central Obesity with Spinopelvic Alignment Parameters in a Chinese Population: A Prospective Study. World Neurosurg 189:e153–e161. https://doi.org/10.1016/j.wneu.2024.06.005
92. Fujimori T et al (2017) The relationship between cervical degeneration and global spinal alignment in patients with adult spinal deformity. Clin Spine Surg 30(4):E423–E429
93. Carpenedo L, Ignasiak D, Remus R, La Barbera L (2025) Advances in Musculoskeletal Modeling of the Thoraco-Lumbar Spine: A Comprehensive Systematic Review. Ann Biomed Eng 53(11):2883–2910
94. Saad E et al (2022) Alteration of the Sitting and Standing Movement in Adult Spinal Deformity, Front. Bioeng. Biotechnol., Volume 9, [Online]. Available: https://www.frontiersin.org/journals/bioengineering-and-biotechnology/articles/ https://doi.org/10.3389/fbioe.2021.751193
95. Rachkidi RE et al (2022) Spinopelvic adaptations in standing and sitting positions in patients with adult spinal deformity. Cureus 14(8):28113

Publisher's Note Springer Nature remains neutral with regard to jurisdictional claims in published maps and institutional affiliations.

Authors and Affiliations

Elisa R. Rosanò[1,2] · Abdul Hulleck[3] · Tao Liu[4] · Marwan El-Rich[3] · Markus Loibl[5] · Fabio Galbusera[5] · Frank Kleinstück[5] · Tamas Fekete[5] · Daniel Haschtmann[5] · Sarah Richner-Wunderlin[5] · Ferran Pellisé[6] · Ibrahim Obeid[7] · Javier Pizones[8] · Ahmet Alanay[9] · Caglar Yilgor[10] · Luigi La Barbera[1] · Stephen J. Ferguson[2] · Dominika Ignasiak[2] · ESSG European Spine Study Group

✉ Elisa R. Rosanò
elisa.rosano@hest.ethz.ch

Abdul Hulleck
abdul.hulleck@ku.ac.ae

Tao Liu
Tao.Liu@ontariotechu.ca

Marwan El-Rich
marwan.elrich@ku.ac.ae

Markus Loibl
Markus.Loibl@kws.ch

Fabio Galbusera
fabio.galbusera@kws.ch

Frank Kleinstück
Frank.Kleinstueck@kws.ch

Tamas Fekete
Tamas.Fekete@kws.ch

Daniel Haschtmann
Daniel.Haschtmann@kws.ch

Sarah Richner-Wunderlin
Sarah.Richner-Wunderlin@kws.ch

Ferran Pellisé
24361fpu@gmail.com

Ibrahim Obeid
ibrahim.obeid@gmail.com

Javier Pizones
javierpizones@gmail.com

Ahmet Alanay
aalanay@gmail.com

Caglar Yilgor
caglaryilgor@gmail.com

Luigi La Barbera
luigi.labarbera@polimi.it

Stephen J. Ferguson
sferguson@ethz.ch

Dominika Ignasiak
dominika.ignasiak@hest.ethz.ch

ESSG European Spine Study Group
europeanspinestudygroup@gmail.com

[1] Laboratory of Biological Structure Mechanics, Department of Chemistry, Materials and Chemical Engineering "Giulio Natta", Politecnico di Milano, Milan, Italy

[2] Institute for Biomechanics, ETH Zurich, Zurich, Switzerland

[3] Khalifa University of Science and Technology, Abu Dhabi, United Arab Emirates

[4] University of Ontario Institute of Technology, Oshawa Ontario, Canada

[5] Schulthess-Klinik, Zurich, Switzerland

[6] Hospital Vall d'Hebron, Barcelona, Spain

[7] Pellegrin Bordeaux University Hospital, Bordeaux, France

[8] Hospital Universitario La Paz, Madrid, Spain

[9] Acibadem University School of Medicine, Istanbul, Turkey

[10] Koc University Hospital Spine Center, Istanbul, Turkey